

# Reduction In Pavement Thickness Using Geogrid - An Economic Approach For NHAI Project

Sagar K. Sonawane<sup>1</sup>, Umair Javed Shaikh<sup>2</sup>, Dr. Rajshekhar G. Rathod<sup>3</sup>, Dr. Yuvaraj L. Bhirud<sup>4</sup>, Dr. Nayeemuddin Mohammed<sup>5</sup>, Dr. Archana G. Tanawade<sup>6</sup>, Dr. Sandeep Sathe<sup>7</sup> and Dr. Shahbaz Dandin<sup>8</sup>

<sup>1,2,3,4</sup>Department of Civil Engineering, School of Engineering and Sciences, MIT Art, Design and Technology University, Pune, Maharashtra, 412201, India

<sup>5</sup>Department of Civil Engineering, Prince Mohammad Bin Fahd University, Al Khobar 31952, Kingdom of Saudi Arabia

<sup>6</sup>Department of Civil Engineering, B.R.A.C.T's Vishwakarma Institute of Technology, Pune, Maharashtra, 411048, India

<sup>7,8</sup>Department of Civil Engineering, Dr. Vishwanath Karad MIT World Peace University, Pune, Maharashtra, 411038, India

sagar.sonawane@mituniversity.edu.in<sup>1</sup>, ushaikh.8711@gmail.com<sup>2</sup>, rajshekhar.rathod@mituniversity.edu.in<sup>3</sup>, yuvaraj.bhirud@mituniversity.edu.in<sup>4</sup>, mnayeemuddin@pmu.edu.sa<sup>5</sup>, archana.tanawade@vit.edu<sup>6</sup>, sandeepsathe@mitwpu.edu.in<sup>7</sup>, shahbaz.dandin@mitwpu.edu.in<sup>8</sup>

<https://orcid.org/0000-0001-6627-0087><sup>1\*</sup>, <https://orcid.org/0000-0002-4582-4025><sup>3</sup>,  
<https://orcid.org/0000-0001-9596-2883><sup>4</sup>, <https://orcid.org/0000-0002-7757-936X><sup>5</sup>,  
<https://orcid.org/0000-0001-5923-2242><sup>6</sup>, <https://orcid.org/0000-0003-2308-4844><sup>7</sup>,  
<https://orcid.org/0000-0003-1471-471X><sup>8</sup>

---

## Abstract

*This research examines the National Highways Authority of India (NHAI) seeks cost-effective and sustainable solutions to improve pavement performance while reducing construction costs. This study explores the structural and economic benefits of integrating geogrid reinforcement in flexible pavements, focusing on optimizing layer thickness without compromising strength. Using mechanistic-empirical analysis, the research compares conventional (IRC 37 compliant) and geogrid-reinforced designs, evaluating subgrade strength, traffic loads and material properties. Findings reveal that geogrids can reduce pavement thickness by 15-25%, yielding significant cost savings through material efficiency, faster construction and enhanced longevity. The study advocates geogrid adoption as a sustainable solution, supporting India's infrastructure development and resource optimization goals.*

**Keywords:** National Highways Authority of India (NHAI), Bituminous Concrete (BC), Wet Mix Macadam (WMM), Mechanistic-Empirical Analysis, Modified Improvement Factor and Layer Coefficient Method.

---

## INTRODUCTION

India's rapid economic growth has increased the demand for high-quality transportation infrastructure [1]. To meet this need, the Government of India (GoI) has launched large-scale highway projects under the National Highway Development Program (NHDP) to improve connectivity and boost economic development. However, rising traffic volumes and heavier axle loads pose challenges for conventional flexible pavements, which rely on thick granular layers for load distribution, leading to higher costs and longer construction time [2]. To overcome these challenges, geosynthetic reinforcement particularly, geogrids has emerged as a sustainable solution [3]. Geogrids are high-strength polymer grids that enhance pavement stability, allowing for reduced layer thickness while maintaining structural integrity. They improve load distribution, prevent crack propagation and increase pavement lifespan by stabilizing subgrades and enhancing drainage. This study evaluates the economic and structural benefits of geogrid-reinforced pavements, focusing on cost savings, construction efficiency and long-term performance for India's highway network. Road maintenance or maintenance of any project is a critical aspect of infrastructure management that directly impacts safety, economic efficiency and long-term performance [4]. In conventional pavement systems, the absence of proper reinforcement often leads to rapid deterioration through mechanisms such as rutting, cracking and pothole formation [5]. These distresses

typically stem from inadequate load distribution, poor subgrade support and water infiltration - all of which significantly increase maintenance requirements and costs [5]. The NHAI faces substantial challenges in maintaining its vast network of highways, where traditional repair approaches often prove costly and temporary in nature. Geogrid-reinforced pavements present a transformative solution to these maintenance challenges. By incorporating geogrids within the pavement structure, engineers can achieve superior load distribution, reduced stress on subgrade layers and enhanced structural integrity. The three-dimensional geogrid matrix effectively interlocks with aggregate materials, creating a stabilized composite structure that resists deformation under traffic loads. This reinforcement mechanism dramatically reduces common pavement distresses, particularly rutting in the wheel paths and reflective cracking from subgrade movements [6]. Laboratory tests and field performance data demonstrate that geogrid-reinforced sections can extend pavement life by 30-50% compared to conventional designs, while simultaneously reducing required maintenance interventions. The economic implications of this technology are particularly significant for NHAI projects. While the initial construction cost may be marginally higher (typically 5-8%), the long-term savings in maintenance expenses are substantial. Studies indicate that properly designed geogrid-reinforced pavements can reduce lifecycle maintenance costs by 25-40% over a 20-year period. These savings accrue from multiple factors reduced frequency of resurfacing, minimized emergency repairs, and extended intervals between major rehabilitations. Furthermore, the reduced maintenance requirements translate to fewer traffic disruptions, lower user delay costs and improved road safety - all critical considerations for India's growing transportation network. From a sustainability perspective, geogrid reinforcement aligns perfectly with modern infrastructure development goals. The technology enables significant reductions in aggregate consumption (typically 15-30% thickness reduction in base courses), thereby conserving natural resources and reducing construction-related emissions. This approach supports NHAI's commitment to environmentally responsible infrastructure while meeting the demanding performance requirements of India's highway network. The integration of geogrids also provides climate resilience, particularly in weak subgrade conditions where conventional pavements are most vulnerable to moisture-related damage. Implementation of geogrid technology follows well-established guidelines in IRC SP:59 [7], which provides comprehensive recommendations for material selection, design methodologies and construction practices. Case studies from various NHAI projects demonstrate successful applications where geogrid reinforcement has delivered exceptional performance in challenging conditions, including high rainfall areas, expansive soils and heavy freight corridors. These real-world examples provide compelling evidence for broader adoption of this technology across India's highway system. This study investigates the role of geogrid reinforcement in flexible pavements as a solution to the NHAI's ongoing challenges related to high construction costs, overuse of materials and early pavement deterioration. The study compares conventional IRC 37 [8] designs with geogrid-reinforced through thickness optimization by mechanistic-empirical analysis and economic assessment.

#### **NHAI Project Site**

The Ministry of Road Transport & Highways (MoRTH) and the NHAI ("the Authority") are actively involved in the development of national highways. As part of this initiative, the Authority has planned to carry out the rehabilitation and enhancement of the design and construction of VUP facilities at four specific locations viz. (i) Kikvi Village (Km 801+080) (ii) Harischandri (Km 806+020) (iii) Shivare (km 817+360) (iv) Khed Shivapur (km 820+340) and FOB at 863+200 on Pune-Satara section of NH-4 from km 725.000 to 865+350 in the state of Maharashtra on EPC mode as shown in Figure 1. The site of the project highway is Pune-Satara section of NH-4 from km 725+000 to 865+350. The project is removal of at grade junctions from national highway and construction VUPs and FOB in rural and urban areas on the completed section of NH-4 on Pune-Satara section in Bhore & Haveli talukas in Pune district road.

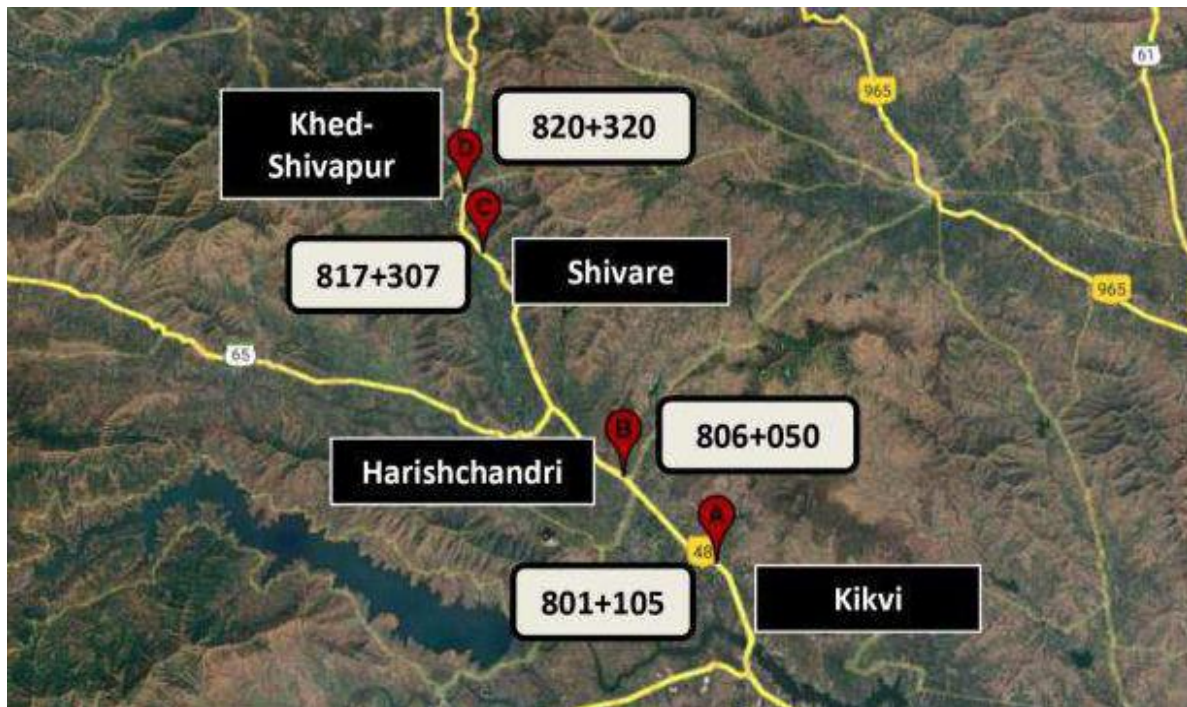


Fig. 1 Study area - all four road stretches (Source: Google Earth)

### 3. Objectives of Study

- To analyze the structural benefits of geosynthetics (geogrids) in reducing pavement thickness while maintaining required strength and durability.
- To compare conventional and geosynthetic-reinforced pavement designs in terms of construction costs, material savings, and long-term maintenance expenses
- To assess the approval process and compliance requirements for using geosynthetics in NHAI highway projects.
- To compare conventional IRC 37 designs with geosynthetic-modified designs.

### 4. Major Key Components as per IRC SP 59

**Geogrid Functionality:** Geogrids play a critical role in pavement reinforcement by enhancing the structural integrity and stability of geotechnical layers. Their primary function is to improve load distribution and confinement within the pavement system, thereby reducing deformation and extending pavement life. For design and application purposes, geogrid properties are broadly categorized into physical, mechanical, and endurance characteristics [7].

**Physical Characteristics:** Physical properties define the geometric and structural configuration of geogrids, including parameters such as aperture size, rib width, junction configuration, thickness, and pattern geometry. These attributes directly influence the interlocking behavior with surrounding aggregates and can be accurately determined using standard measurement procedures [7].

**Mechanical Characteristics:** Mechanical properties are crucial as they relate to the geogrid's ability to resist tensile forces during installation and service life. Key parameters include tensile strength at both the ribs and junctions. Testing methods such as the single rib tensile test and wide-width tensile test are commonly used to evaluate these properties. The single rib test involves pulling individual longitudinal or transverse ribs (based on geogrid orientation) to failure under controlled extension, following ASTM D6637 [9] procedures. For more comprehensive assessment, wide-width testing (as per ISO 10319, IS 13325, or ASTM D6637) evaluates the collective tensile behavior across multiple ribs [7].

Table 1 Laboratory test result of geogrid

Test Parameter	Results
Single Rib tensile strength strain (kN/m)	

Machine Direction (kN/m)	49.6
Cross Machine Direction (kN/m)	48.9
Elongation @ designated Load (%)	
Machine Direction @ 40 (KN/m)	8.9
Cross Machine Direction @ 40 (KN/m)	10.8

**Laboratory Test Results of Geogrid:** The geogrid was tested at The Bombay Textile Research Association (BTRA), an approved laboratory under the Ministry of Textiles, Government of India, located at Lal Bahadur Shastri Marg, Ghatkopar (West), Mumbai - 400086.

Testing was conducted on 12<sup>th</sup> February 2025 in accordance with IRC guidelines, with reference to Table 1 for evaluation criteria. All test results mentioned in Table 1 were found to be within specified limits, confirming the geogrid's compliance with the required mechanical properties for pavement reinforcement applications.

**Endurance Characteristics:** Given their role in long-term infrastructure, geogrids must also withstand prolonged exposure to mechanical, environmental, and installation-related stresses [7].

**Installation Damage:** Physical handling and heavy equipment can damage geogrids if not properly managed. Standardized methods such as ISO 10722 and ASTM D5818 are used to evaluate post-installation integrity. Use of cushioning layers, such as sand, is recommended in high-impact areas to prevent tearing from coarse aggregates or mechanical loading [7].

**Creep Behavior:** Geogrids are subject to time-dependent deformation under constant load, known as tensile creep. This behavior is influenced by polymer type, stress level, temperature, and duration of load application. Test methods including ISO 13431, ASTM D6992, and ASTM D5262 are employed to evaluate long-term tensile creep. Creep reduction factors for design are referenced from IRC SP 102 and MoRTH Section 3100 [7].

**Degradation Resistance:** Environmental conditions such as temperature and oxidation can impact geogrid performance over time. While typical service temperatures are not detrimental, prolonged exposure to high temperatures can exacerbate creep. Oxidation resistance, particularly for polypropylene and polyethylene geogrids, is assessed using EN ISO 13438 standards to ensure material stability during the design life [7].

**Pavement Design:** The pavement design for this project is carried out in accordance with IRC SP 59 [7] and IRC 37 [8]. These codes provide standardized methodologies to ensure durable and cost-effective pavements tailored to Indian traffic and climatic conditions.

IRC SP 59 focuses on empirical design for low-to-medium traffic volumes (typically <30 MSA). It uses California Bearing Ratio (CBR) for subgrade strength assessment which is suitable for rural roads, urban streets, and highways with lighter traffic and IRC 37 adopts a mechanistic-empirical approach for high-traffic highways (>30 MSA). It considers fatigue and rutting failures based on layer material properties and preferred for national highways, expressways, and heavy-duty corridors. By integrating both codes, the design optimizes performance for varying traffic loads and site-specific conditions along the Pune-Satara corridor.

## 5. Problem Statement

A contractor has been awarded a National Highway project after quoting 30% below the estimated cost, making cost-efficiency essential for maintaining project viability. The highway experiences high traffic volumes exceeding 3,000 Commercial Vehicles per Day (CVPD), including heavy axle loads that accelerate pavement deterioration. Compounding the issue are poor drainage conditions, which further compromise pavement performance and demand increased structural thickness. Given the financial constraints and performance requirements, traditional design approaches become economically

unsustainable. Therefore, innovative and cost-effective engineering solutions are essential. The integration of geosynthetics, particularly geogrids, offers a viable alternative by improving the structural integrity of the pavement, enabling reduced layer thickness without compromising durability or service life.

## LITERATURE REVIEW

Early research by Vennamaneni et al. demonstrated that placing one or more biaxial geogrid layers in a weak lateritic subgrade can markedly raise its California Bearing Ratio (CBR), translating to thinner design thickness. In soaked CBR tests, a double geogrid in the subgrade yielded a 21.3% reduction in pavement thickness required for a low-volume road, compared to an unreinforced design [10]. Similarly, Sivapriya and Ganesh-Kumar reinforced a clay subgrade with up to three geogrid layers in CBR molds and found steadily increasing CBR values with each additional layer. The optimal geogrid configuration led to an estimated 6–7% reduction in the required pavement crust thickness, alongside a modest cost benefit [11]. These studies confirm that even at the subgrade level, geogrids substantially improve support capacity, permitting thinner overlying layers. Goud et al. adopted Indian mechanistic design guidelines (IRC 37:2018) to develop geogrid-specific design charts based on Layer Coefficient Ratio (LCR) and Traffic Benefit Ratio (TBR) values. They report that for a given traffic level and subgrade strength, incorporating a geogrid in the base can reduce the required aggregate base thickness by about 28–45%. Notably, larger thickness reductions were achieved on weaker subgrades (CBR < 5%) where the geogrid's contribution is most needed [12]. In the same vein, Baadiga and Balunaini performed large-scale tests on soft clay subgrades (CBR 2–5%) with different geogrid types. They quantified significant increases in effective subgrade CBR (from 2.5% up to ~10–11% when stabilized with a stiff geogrid) and reported Layer Coefficient Ratios in the range of 1.3–1.6 for geogrid-reinforced base layers [13]. In practical terms, these LCR values indicate that a geogrid-stabilized base can be about one-third thinner than a conventional base for the same structural capacity [13]. In fact, an earlier model by Saride et al. predicted roughly 33% reduction in base course thickness when using a high-strength geogrid, consistent with these experimental findings [14]. Abu-Farsakh et al. found that a 457 mm-thick base course could be reduced by approximately one-third with a single geogrid at the base–subgrade interface, with no loss in performance [15]. Al-Qadi et al. conducted accelerated pavement tests on nine instrumented sections and confirmed that geogrid reinforcement can decrease required base thickness on the order of 10–40%, depending on geogrid placement and subgrade stiffness [16]. In one section with a relatively strong subgrade, a modest ~7% base reduction was achievable with geogrid reinforcement [17], whereas sections on weaker subgrades saw much larger reductions. A comprehensive field trials review by Alimohammadi et al. concluded that the magnitude of thickness reduction (or equivalently, the structural number reduction) due to geosynthetics depends on various factors – especially subgrade CBR and base course quality – but double-digit percentage savings in aggregate layer thickness are routinely observed when geogrids are properly applied [18]. These savings are particularly valuable given the scarcity of quality aggregates in many regions [12]. Bodhanam et al. performed a cost analysis alongside large-scale tests on pavements with subgrade CBR 6–10%. They found geogrid-reinforced designs saved 14–24% in total material costs compared to the conventional design [19]. The largest savings were seen for the weakest subgrade (CBR 6%) reinforced with a high-strength PET geogrid, which yielded nearly one-quarter reduction in cost [19]. In another study focused on subgrade reinforcement, Sivapriya & Ganesh-Kumar noted about a 6.4% reduction in initial construction cost by using an optimal geogrid layer in the subgrade [11]. While this percentage is smaller, the study targeted only subgrade improvement; larger savings would accrue if the base and sub-base were also optimized. Research converges on placing geogrids at the interface of the base and subgrade for maximum benefit, especially in thick base sections. This position provides stabilization of the weak subgrade and prevents contamination of base aggregates. For thinner base courses (< 200 mm), some recommend placing the geogrid at mid-depth of the base layer [20, 21]. The literature consistently supports geogrid adoption as a cost-effective, sustainable strategy for strengthening flexible pavements. Embracing this technology will help optimize resources and improve the longevity of India's road infrastructure, fulfilling the twin objectives of economic efficiency and performance resilience [21] in NHAI projects.

## METHODOLOGY

The figure 2 gives the methodology adopted for present study and steps in geogrid pavement design.

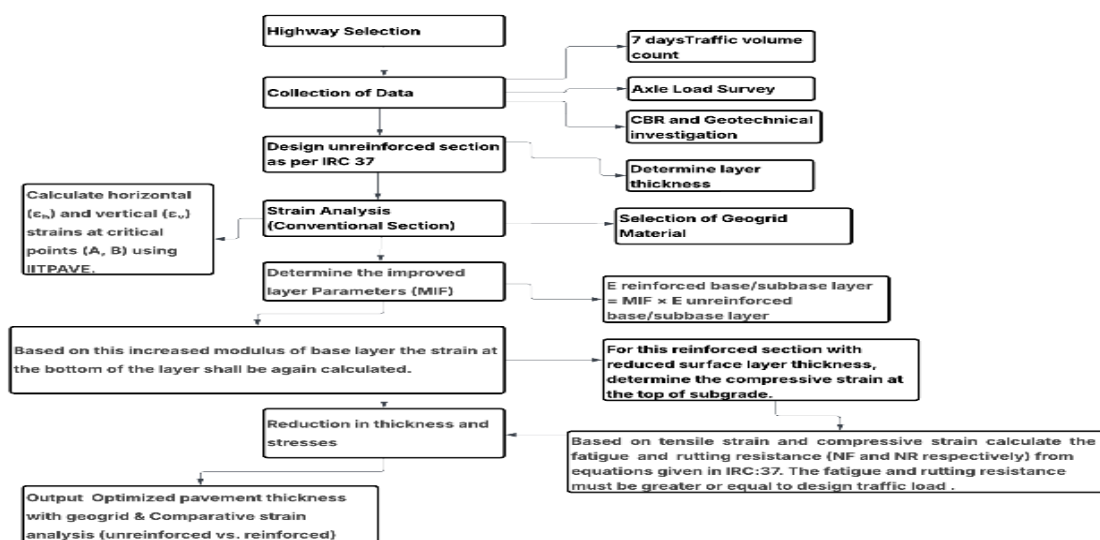


Fig. 2 Flowchart for design of geogrid pavements

### Demography of Study Area

The study focuses on the Pune-Satara section of NH-4, spanning from km 725+000 to 865+350. The project involves the removal of at-grade junctions from the national highway and the construction of Vehicular Underpasses (VUPs) and Foot Overbridges (FOBs) in both rural and urban areas along the completed section of NH-4 in the Bhore and Haveli talukas of Pune district.

### Data Collection

The data collection is carried out based on the factors to be considered for analysis. As mentioned, the traffic varies daily, monthly and seasonally. The data is collected throughout the week that is from 16<sup>th</sup> April, 2024 to 22<sup>nd</sup> April 2024.

### Primary Data Collection

The primary data was obtained through an axle load survey conducted at the designated highway location, with data recorded separately for each direction at all study sites. The seven days traffic volume count is taken near Khed Shivapur toll plaza and results are shown in Table 2. The toll reports are extracted month-wise to understand the monthly variation of traffic.

Table 2 Summary of commercial vehicle count

Sr. No.	Type of Vehicle	Average Daily Traffic
1	Mini Bus, Bus	390
2	Tempo/Mini LCV	634
3	LCV	502
4	2 Axle Trucks	2592
5	3 Axle Trucks	277
6	Multi Axle Trucks	382
7	Tractor with Trailer & Without trailer	4
	Commercial Vehicles per day (CVPD)	4781

### Secondary Data Collection

The secondary data necessary for this study includes the traffic growth rate, subgrade CBR value, and details of the existing pavement layers, as presented in Table 3. Based on soil investigations carried out

along the project road and the presence of suitable borrow material in the region, the strength of borrow areas is estimated to range between 15% and 18% across different highway sections. Accordingly, an average CBR value of 12% has been adopted for the design.

Table 3 Summary of soil test report

Chainage (CH)	Atterberg Limit			Grain Size Analysis			CBR
	LL	PL	FSI	Gravel	Sand	Silt	
Unit	-	-	%	%	%	%	%
820+340	NP	NP	13	24.2	53.5	22	18.5
817+340	39	24	33	42.1	21.8	36	15

#### Pavement Layer as per Contract Agreement

The design of flexible pavements, whether for new construction, widening, strengthening, or approach roads shall be based on a minimum design life of 20 years, assuming an effective subgrade CBR of 12% and a minimum design traffic of 100 million standard axles.

#### Approach used for the Study:

It includes the fatigue and rutting strains obtained from the specified stretches by using geogrid in the pavement. The fatigue and rutting (deformation) for main carriageway and service road, and also checking of allowable horizontal tensile strain bottom of bituminous layer and allowable vertical compressive strain at top of subgrade layer in unreinforced layer system and for reinforced layer system.

##### a. Subgrade rutting criteria

$$NR = 1.4100 \times 10^{-08} (1/E_v)^{4.5337}$$

NR = subgrade rutting life (cumulative equivalent number of 80 kN standard axle loads that can be served by the pavement before the critical rut depth of 20 mm or more occurs)

$E_v$  = vertical compressive strain at the top of the subgrade calculated using linear elastic layered theory by applying standard axle load at the surface of the selected pavement system [8].

##### b. Fatigue cracking criteria for bituminous layer

$$N_f = 0.5161 \cdot C \cdot 10^{-04} [1/\epsilon_t] 3.89 [1/MR_m]^{0.854}$$

$N_f$  = fatigue life of bituminous layer (cumulative equivalent number of 80 kN standard axle loads that can be served by the pavement before the critical cracked area of 20% or more of paved surface area occurs)

$\epsilon_t$  = maximum horizontal tensile strain at the bottom of the bottom bituminous layer (DBM) calculated using linear elastic layered theory by applying standard axle load at the surface of the selected pavement system.

$MR_m$  = resilient modulus (MPa) of the bituminous mix used in the bottom bituminous layer, selected as per the recommendations made in these guidelines [8].

## CALCULATIONS, RESULTS AND ANALYSIS

This section presents the fatigue and rutting strain analysis derived from specific highway stretches where geogrids have been incorporated into the pavement structure. It includes a detailed assessment of permissible strain limits, both fatigue and rutting; for the main carriageway and service road. The evaluation involves checking the allowable horizontal tensile strain at the bottom of the bituminous layer and the allowable vertical compressive strain at the top of the subgrade, under both unreinforced and geogrid-reinforced pavement configurations, using output generated from IITPAVE software. A comparative analysis of fatigue and rutting strains is conducted to highlight the performance enhancement due to geogrid inclusion. Additionally, the calculation of the modified resilient modulus for reinforced layers is detailed, providing insights into structural improvement. The analysis follows the methodologies outlined in Section 7.

### A. Calculation and results of permissible strains for main carriageway

#### 1. Calculation of conventional section:



For the pavement composition as stated above the equations NR & Nf of IRC 37 are used to calculate the allowable stains.

- Allowable horizontal tensile strain bottom of bituminous layer =  $142 \times 10^6$
- Allowable vertical compressive strain at top of subgrade layer =  $318 \times 10^6$ .

Based on the IIT pave analysis shown in figure 3, the following stresses are calculated.

No. of layers	3								
E values (MPa)	3000.00	269.87	86.33						
Mu values	0.350	0.350	0.35						
thicknesses (mm)	90.00	450.00							
single wheel load (N)	20000.00								
tyre pressure (MPa)	0.56								
Dual Wheel									
Z	R	SigmaZ	SigmaT	SigmaR	TaoRZ	DispZ	epZ	epT	epR
90.00	0.00	-0.2140E+00	0.8918E+00	0.7203E+00	-0.1893E-01	0.3977E+00	-0.2594E-03	0.2382E-03	0.1610E-03
90.00L	0.00	-0.2140E+00	-0.2463E-01	-0.4007E-01	-0.1893E-01	0.3977E+00	-0.7090E-03	0.2382E-03	0.1610E-03
90.00	155.00	-0.1524E+00	0.5959E+00	-0.2907E-01	-0.9524E-01	0.4003E+00	-0.1169E-03	0.2198E-03	-0.6144E-04
90.00L	155.00	-0.1524E+00	-0.2106E-01	-0.7728E-01	-0.9524E-01	0.4003E+00	-0.4371E-03	0.2198E-03	-0.6144E-04
540.00	0.00	-0.2525E-01	0.3726E-01	0.3127E-01	-0.4499E-02	0.2557E+00	-0.1824E-03	0.1303E-03	0.1003E-03
540.00L	0.00	-0.2540E-01	0.2595E-02	0.6858E-03	-0.4499E-02	0.2556E+00	-0.3075E-03	0.1303E-03	0.1004E-03
540.00	155.00	-0.2749E-01	0.4015E-01	0.3602E-01	-0.6471E-02	0.2637E+00	-0.2006E-03	0.1377E-03	0.1170E-03
540.00L	155.00	-0.2749E-01	0.2784E-02	0.1445E-02	-0.6357E-02	0.2637E+00	-0.3356E-03	0.1378E-03	0.1169E-03

Fig. 3 Critical Points for Evaluation of Horizontal and Vertical Strains

- Actual horizontal tensile strain at bottom of bituminous layer =  $139.1 \times 10^6$
- Actual vertical compressive strain at top of subgrade layer =  $205.4 \times 10^6$

## 2. Calculation of reinforced section:

- Resilient modulus of subgrade
- Subgrade CBR = 12%
- MR subgrade =  $17.6 \times \text{CBR}^{0.64} = 17.6 \times 120.64 = 86.34 \text{ MPa}$
- Resilient modulus of granular sub-base layer
- Thickness of GSB layer = 180 mm
- MR GSB =  $0.2 \times \text{MR subgrade} \times h^{0.45} = 0.2 \times 86.34 \times 1800.45 = 178.69 \text{ MPa}$
- Effective modulus of subgrade and GSB layer
- The effective modulus of subgrade and 180 mm thick GSB layer is estimated using equation 6.3 of IRC 37-2018 as follows

- $M_{RS} = \frac{2(1-\mu)p_a}{\delta}$
- Where, p = contact pressure = 0.56 MPa
- a = radius of circular contact area = 150.8 mm
- $\mu$  = Poisson's ratio = 0.35
- $\delta$  = maximum surface deflection obtained from IITPAVE software considering a single wheel load of 40,000 N and a contact pressure of 0.56 MPa.

No. of layers	2								
E values (MPa)	178.64	86.34							
Mu values	0.350	0.35							
thicknesses (mm)	180.00								
single wheel load (N)	40000.00								
tyre pressure (MPa)	0.56								
Single Wheel									
Z	R	SigmaZ	SigmaT	SigmaR	TaoRZ	DispZ	epZ	epT	epR
0.00	0.00	-0.5525E+00	-0.5723E+00	-0.5723E+00	0.0000E+00	0.1216E+01	-0.8506E-03	-0.9997E-03	-0.9997E-03

Fig. 4 Output of IIT Pave for Delta

No. of layers	4								
E values (MPa)	3000.00	375.85	178.69	86.34					
Mu values	0.350	0.350	0.350	0.35					
thicknesses (mm)	160.00	100.00	100.00						
single wheel load (N)	20000.00								
tyre pressure (MPa)	0.56								
Dual Wheel									
Z	R	SigmaZ	SigmaT	SigmaR	TaoRZ	DispZ	epZ	epT	epR
160.00	0.00	-0.1122E+00	0.5288E+00	0.4198E+00	-0.2018E-01	0.3193E+00	-0.1477E-03	0.1394E-03	0.9158E-04
160.00L	0.00	-0.1122E+00	0.1301E-01	-0.3116E-03	-0.2018E-01	0.3193E+00	-0.3105E-03	0.1394E-03	0.9158E-04
160.00	155.00	-0.9511E-01	0.4695E+00	0.2336E+00	-0.6415E-01	0.3279E+00	-0.1137E-03	0.1403E-03	0.3419E-04
160.00L	155.00	-0.9511E-01	0.1402E-01	-0.1553E-01	-0.6415E-01	0.3279E+00	-0.2517E-03	0.1403E-03	0.3419E-04
320.00	0.00	-0.2180E-01	0.1734E-01	0.1448E-01	-0.3586E-02	0.2425E+00	-0.1849E-03	0.1114E-03	0.8992E-04
320.00L	0.00	-0.2180E-01	0.2301E-02	0.9268E-03	-0.3586E-02	0.2425E+00	-0.2460E-03	0.1114E-03	0.8992E-04
320.00	155.00	-0.2330E-01	0.1852E-01	0.1651E-01	-0.4903E-02	0.2487E+00	-0.1990E-03	0.1170E-03	0.1018E-03
320.00L	155.00	-0.2330E-01	0.2468E-02	0.1493E-02	-0.4883E-02	0.2487E+00	-0.3859E-03	0.1170E-03	0.1017E-03

Fig. 5 Output of IIT Pave for stress calculation.

Based on the IIT pave analysis shown in figure 4 & 5, the following stresses are calculated.



- Actual horizontal tensile strain at bottom of bituminous layer as per fig. 4 =  $139.1 \times 10^6$
- Actual vertical compressive strain at top of subgrade layer as per fig. 5 =  $205.4 \times 10^6$

Table 4 Summary of pavement thickness for main carriageway

Type of Layer	Conventional Thickness (mm)	Reinforced
		Thickness (mm)
BC	50	40
DBM	125	120
WMM	250	180
GSB	200	180

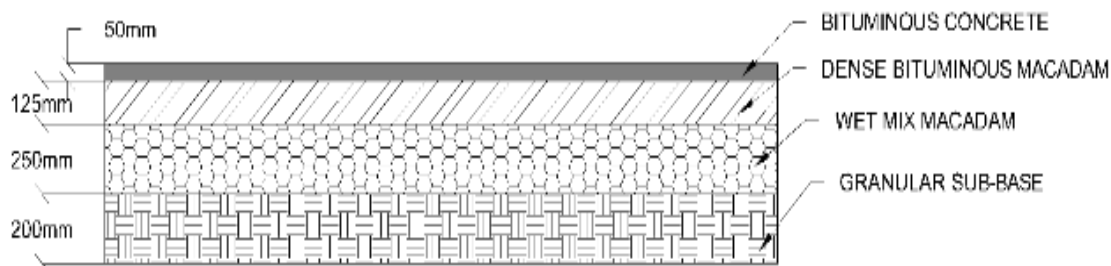


Fig. 6 Cross section for conventional section

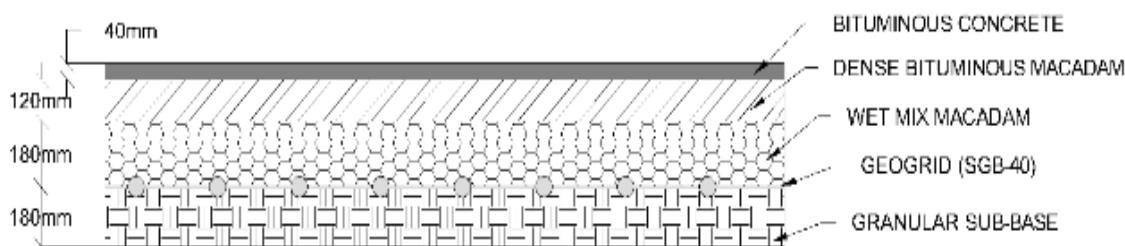


Fig. 7 Cross section for reinforced section

The table 4 gives the pavement thickness for main carriageway and figures 6 & 7 shows the sections for conventional & reinforced section for main carriageway respectively.

## B. Calculation and results of permissible strains for service road

### 1. Calculation of conventional section:

For the pavement composition as stated above the equation NR & Nf of IRC 37 are used to calculate the allowable strains.

- Allowable horizontal tensile strain bottom of bituminous layer =  $263.1 \times 10^6$
- Allowable vertical compressive strain at top of subgrade layer =  $577.7 \times 10^6$

Based on the IIT pave analysis, the following stresses are calculated as shown in figure 8.

No. of layers	3								
E values (MPa)	3000.00	269.87	86.33						
Mu values	0.350	0.350	0.35						
thicknesses (mm)	90.00	450.00							
single wheel load (N)	20000.00								
tyre pressure (MPa)	0.56								
Dual Wheel									
Z	R	SigmaZ	SigmaT	SigmaR	TaoRZ	DispZ	epZ	epT	epR
90.00	0.00-0.2140E+00	0.8918E+00	0.7203E+00-0.1893E-01	0.3977E+00-0.2594E-03	0.2382E-03	0.1610E-03			
90.00L	0.00-0.2140E+00-0.2463E-01-0.4007E-01-0.1893E-01	0.3977E+00-0.7090E-03	0.2382E-03	0.1610E-03					
90.00	155.00-0.1524E+00	0.5959E+00-0.2907E-01-0.9524E-01	0.4003E+00-0.1169E-03	0.2198E-03-0.6144E-04					
90.00L	155.00-0.1524E+00-0.2106E-01-0.7728E-01-0.9524E-01	0.4003E+00-0.4371E-03	0.2198E-03-0.6144E-04						
540.00	0.00-0.2525E-01	0.3726E-01	0.3127E-01-0.4499E-02	0.2557E+00-0.1824E-03	0.1303E-03	0.1003E-03			
540.00L	0.00-0.2540E-01	0.2595E-02	0.6858E-03-0.4499E-02	0.2556E+00-0.3075E-03	0.1303E-03	0.1004E-03			
540.00	155.00-0.2749E-01	0.4015E-01	0.3602E-01-0.6471E-02	0.2637E+00-0.2006E-03	0.1377E-03	0.1170E-03			
540.00L	155.00-0.2749E-01	0.2784E-02	0.1445E-02-0.6357E-02	0.2637E+00-0.3356E-03	0.1378E-03	0.1169E-03			

Fig. 8 Critical points for evaluation of horizontal and vertical strains using IITpave

- Actual horizontal tensile strain at bottom of bituminous layer =  $238.2 \times 10^6$
- Actual vertical compressive strain at top of subgrade layer =  $335.6 \times 10^6$

### 2. Calculation of reinforced section

#### Detailed Calculations for Main Carriageway

- Resilient modulus of subgrade
- Subgrade CBR = 12%
- MR subgrade =  $17.6 \times \text{CBR}^{0.64} = 17.6 \times 120.64 = 86.34 \text{ MPa}$
- Resilient modulus of granular sub-base layer
- Thickness of GSB layer = 180 mm
- MR GSB =  $0.2 \times \text{MR subgrade} \times h^{0.45} = 0.2 \times 86.34 \times 1800.45 = 178.69 \text{ MPa}$
- Effective modulus of subgrade and GSB layer
- The effective modulus of subgrade and 180 mm thick GSB layer is estimated using equation 6.3 of IRC 37-2018 as follows
- $\text{MRS} = \frac{2(1-\mu^2)p_a}{\delta}$
- Where, p = contact pressure = 0.56 MPa
- a = radius of circular contact area = 150.8 mm
- $\mu$  = Poisson's ratio = 0.35
- $\delta$  = maximum surface deflection obtained from IITPAVE software considering a single wheel load of 40,000 N and a contact pressure of 0.56 MPa.

```

No. of layers          2
E values (MPa)        178.64  86.34
Mu values              0.350.35
thicknesses (mm)      180.00
single wheel load (N) 40000.00
tyre pressure (MPa)   0.56
Single Wheel
Z      R      SigmaZ      SigmaT      SigmaR      TacRZ      DispZ      epZ      epT      epR
0.00   0.00 -0.5525E+00 -0.5723E+00 -0.5723E+00 0.0000E+00 0.1216E+01 -0.8506E-03 -0.9997E-03 -0.9997E-03

```

Fig. 9 Output of IITpave for delta

```

No. of layers          4
E values (MPa)        3000.00  374.98  178.68  86.33
Mu values              0.350.350.350.35
thicknesses (mm)      30.00  180.00  180.00
single wheel load (N) 20000.00
tyre pressure (MPa)   0.56
Single Wheel
Z      R      SigmaZ      SigmaT      SigmaR      TacRZ      DispZ      epZ      epT      epR
30.00   0.00 -0.5229E+00 0.4078E+00 0.4081E+00 0.0000E+00 0.3938E+00 -0.2695E-03 0.1493E-03 0.1495E-03
30.00L 0.00 -0.5229E+00 -0.1954E+00 -0.1953E+00 0.0000E+00 0.3938E+00 -0.1030E-02 0.1493E-03 0.1495E-03
30.00  155.00 -0.4270E-01 -0.8958E-01 -0.5201E+00 -0.7716E-01 0.2501E+00 0.5689E-04 0.3580E-04 -0.1579E-03
30.00L 155.00 -0.4270E-01 -0.3132E-01 -0.8513E-01 -0.7716E-01 0.2501E+00 -0.5193E-05 0.3580E-04 -0.1579E-03
390.00   0.00 -0.3106E-01 0.2463E-01 0.2453E-01 0.0000E+00 0.1963E+00 -0.2701E-03 0.1506E-03 0.1499E-03
390.00L 0.00 -0.3105E-01 0.3315E-02 0.3145E-02 0.0000E+00 0.1963E+00 -0.3859E-03 0.1515E-03 0.1489E-03
390.00  155.00 -0.2440E-01 0.1959E-01 0.1456E-01 -0.7981E-02 0.1814E+00 -0.2034E-03 0.1289E-03 0.9090E-04
390.00L 155.00 -0.2439E-01 0.2681E-02 0.2589E-03 -0.7974E-02 0.1814E+00 -0.2945E-03 0.1289E-03 0.9103E-04

```

Fig. 10 Output of IITpave for stress calculation

Based on the IIT pave analysis shown in figures 9 & 10, the following stresses are calculated.

- Actual horizontal tensile strain at bottom of bituminous layer =  $139.1 \times 10^{-6}$
- Actual vertical compressive strain at top of subgrade layer =  $205.4 \times 10^{-6}$ .

Table 5 Summary of pavement thickness for service carriageway

Type of Layer	Conventional Thickness (mm)	Reinforced
		Thickness (mm)
BC	40	30
DBM	55	0
WMM	250	180
GSB	200	180

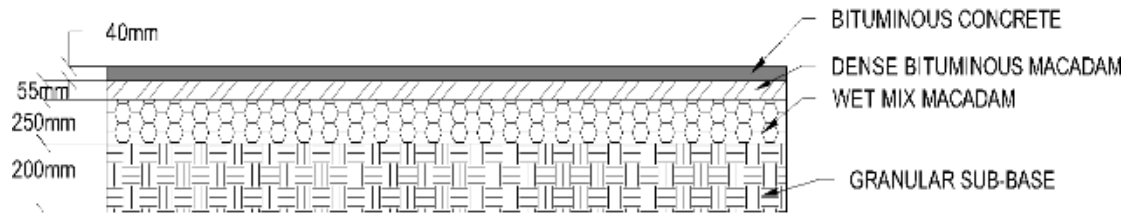


Fig. 11 Cross section for conventional section service road

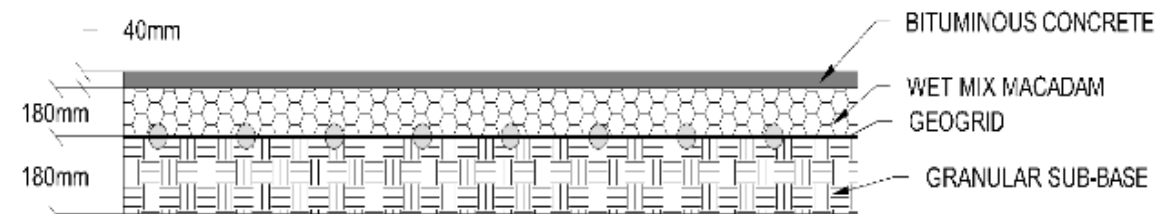


Fig. 12 Cross section for reinforced section service road

The table 5 gives the pavement thickness for service road and figures 11 & 12 shows the sections for conventional & reinforced section for service road respectively.

### 3. Comparison for reduction in thickness:

Table 6 Summary of pavement thickness reduction

Main Carriageway			
Layer	Conventional (mm)	Reinforced Thickness (mm)	% Reduction
BC	50	40	20
DBM	125	120	4
WMM	250	180	28
GSB	200	180	10
		Average reduction	15.5
Service Road			
Layer	Conventional (mm)	Reinforced Thickness (mm)	% Reduction
BC	40	30	25
DBM	55	0	100
WMM	250	180	28
GSB	200	180	10
		Average reduction	40.75

The comparison between conventional and reinforced pavement layers for both the main carriageway and service road demonstrates significant reductions in layer thickness due to reinforcement and given in Table 6.

### 4. Cost comparison conventional and reinforced section

The comparison of cost estimates is conducted to assess optimization. The comparison between conventional pavement and the geogrid-reinforced section is performed using Strata Grid™ SGB40 and rates as per SSR 2022 / 2023. The layers of both conventional and reinforced sections are detailed in the table 7. Significant cost savings are achieved by using geogrid, and the use of traditional materials such as aggregates can be reduced accordingly.

Table 7 Summary of cost comparison

Type	Main Road	Service Road
Conventional Section	17.07 Cr	8.67 Cr
Reinforced section	15.89 Cr	6.31 Cr
Difference	1.18 Cr	2.36
Cost Variation	13.52%	

Table 7 present the total estimated costs for conventional pavement and pavement reinforced with geogrid. The data in these tables demonstrate that using geogrid can result in potential cost savings of up to 13.52% compared to conventional pavement.

## CONCLUSION

The findings demonstrate that incorporating geogrid reinforcement significantly enhances pavement performance while optimizing material usage and construction costs. The reinforced sections exhibited lower horizontal tensile strains at the bottom of the bituminous layer and reduced vertical compressive strains at the subgrade level compared to conventional sections, ensuring compliance with IRC 37 standards. Reinforcement with Strata Grid™ SGB40 allowed for substantial reductions in layer thickness up to 28% in Wet Mix Macadam (WMM) and 20% in Bituminous Concrete (BC) for the main carriageway and even more significant savings in the service road. The economic analysis revealed a 13.52 % reduction in overall pavement costs due to decreased material requirements and optimized layer thicknesses, translating to substantial project savings. Despite reduced thicknesses, the reinforced sections maintained structural adequacy, as validated by IIT Pave simulations, confirming their safety and durability under design loads. In summary, geogrid reinforcement offers a technically viable and economically advantageous solution for flexible pavement construction. The results validate its effectiveness in enhancing pavement longevity while minimizing resource consumption and construction expenses. These findings support the adoption of geogrid-reinforced pavements in similar infrastructure projects for sustainable and cost-effective road development.

## Future Scope

1. Smart material innovations development of sensor-embedded, nano-enhanced and recycled geogrids for real-time monitoring and sustainable pavement solutions.
2. Expanded applications & standards adaptation for airfields/smart cities, disaster resilience, and establishment of global design guidelines.
3. Long-term durability studies accelerated life testing and chemical degradation research to validate multi-decade performance.

## REFERENCES

- [1] Murde, A.A., Sonawane, S.K., Mulay, H. (2024). Economic Evaluation and Feasibility Studies at Indoli Junction (km. 704/200 of New NH48) Before and After Construction of Flyover. In: Sivakumar Babu, G.L., Mulangi, R.H., Kolathayar, S. (eds) Technologies for Sustainable Transportation Infrastructures. SIIOC 2023. Lecture Notes in Civil Engineering, vol 529. Springer, Singapore. [https://doi.org/10.1007/978-981-97-4852-5\\_20](https://doi.org/10.1007/978-981-97-4852-5_20)
- [2] Gayakwad, A.P., Rathod, R., Sonawane, S. (2024). Black Cotton Soil Stabilization by Using Bio-enzyme and Marble Dust Powder for Pavement Subgrade. In: Sivakumar Babu, G.L., Mulangi, R.H., Kolathayar, S. (eds) Technologies for Sustainable Transportation Infrastructures. SIIOC 2023. Lecture Notes in Civil Engineering, vol 529. Springer, Singapore. [https://doi.org/10.1007/978-981-97-4852-5\\_17](https://doi.org/10.1007/978-981-97-4852-5_17)
- [3] Chipade, A. M., Vispute, P. P., Sonawane, S. K., Sasane, N. B., Jadhav, M., & Nerlekar, T. (2025). Construction Materials for Sustainable Environment in Residential Buildings. *Journal of Mines, Metals and Fuels*, 73(1), 173–188. <https://doi.org/10.18311/jmmf/2025/46248>
- [4] Chipade, A. M., Zolekar, A. R., Sonawane, S. K., Mishra, S., Nerlekar, T., & Londhe, P. (2025). Evolution of Critical Success Factor in Residential Project. *Journal of Mines, Metals and Fuels*, 73(4), 1107–1120. <https://doi.org/10.18311/jmmf/2025/47759>
- [5] Sonawane, S.K., Dwivedi, A. K., Naktode, P. L., (2024). A Comprehensive Systematic Review on the Application of Coal Ash in Bituminous Pavements. *Nanotechnology Perceptions*, 20(15), 3730-3747, <https://doi.org/10.62441/nano-ntp.vi.4672>
- [6] Sonawane, S.K., Dwivedi, A.K. & Naktode, P.L. (2025). Effect of steel fiber and coal ash on the properties of dense bituminous macadam mixes of Indian Roads Congress grading II. *Innov. Infrastruct. Solut.* 10, 147. <https://doi.org/10.1007/s41062-025-01957-4>
- [7] IRC:SP:59 (2019), Guidelines for use of Geosynthetics in Road Pavements and Associated Works, Indian Roads Congress, India.

- [8] IRC:37 (2018), Guidelines for the Design of Flexible Pavements, Indian Roads Congress, India.
- [9] ASTM D6637-11 (2015), Standard Test Method for Determining Tensile Properties of Geogrids by the Single or Multi-Rib Tensile Method, ASTM, US.
- [10] Vennamaneni, S., Aketi, N. R., & Paisa, S. (2018). Reduction in Pavement Thickness by Using Geogrid. *International Journal of Engineering & Technology*, 7(3.3), 17–20. <https://doi.org/10.14419/ijet.v7i3.3.14473>
- [11] Sivapriya, S. V., & Ganesh-Kumar, S. (2019). Functional and Cost-Benefits of Geosynthetics as Subgrade Reinforcement in the Design of Flexible Pavement. *Revista Facultad de Ingenieria*, 28(51), 39–49. <https://doi.org/10.19053/012111129.v28.n51.2019.9082>
- [12] Goud, G. N., Mouli, S. S., Umashankar, B., Sireesh, S., & Madhav, R. M. (2020). Design and Sustainability Aspects of Geogrid-Reinforced Flexible Pavements—An Indian Perspective. *Frontiers in Built Environment*, 6, 71. <https://doi.org/10.3389/fbuil.2020.00071>
- [13] Baadiga, R., & Balunaini, U. (2023). Evaluation of Pavement Design Input Parameters of Biaxial and Triaxial Geogrid Stabilized Flexible Pavements Overlying Soft Subgrades. *Cleaner Materials*, 9(3), 100192. <https://doi.org/10.1016/j.clema.2023.100192>
- [14] Saride S., and Baadiga R., (2020), New Layer Coefficients for Geogrid-Reinforced Pavements Bases, Proceedings of Indian Geotechnical Conference, Andhra University, Visakhapatnam.
- [15] Abu-Farsakh, M., Hanandeh, S., Mohammad, L., & Chen, Q. (2016). Performance of Geosynthetic Reinforced/Stabilized Paved Roads Built Over Soft Soil Under Cyclic Plate Loads. *Geotextiles and Geomembranes*, 44(6), 845–853. <https://doi.org/10.1016/j.geotexmem.2016.06.009>
- [16] Al-Qadi, I. L., Dessouky, S. H., Kwon, J., & Tutumluer, E. (2008). Geogrid in Flexible Pavements: Validated Mechanism. *Transportation Research Record*, 2045(1), 102–109. <https://doi.org/10.3141/2045-12>
- [17] Sharbaf, M. R., & Ghafoori, N. (2021). Laboratory Evaluation of Geogrid-Reinforced Flexible Pavements. *Transportation Engineering*, 4, 1–10. <https://doi.org/10.1016/j.treng.2021.100070>
- [18] Alimohammadi, H., Schaefer, V. R., Zheng, J., & Li, H. (2021). Performance Evaluation of Geosynthetic Reinforced Flexible Pavement: A Review of Full-Scale Field Studies. *International Journal of Pavement Research and Technology*, 14(1), 30–42. <https://doi.org/10.1007/s42947-020-0019-y>
- [19] Bodhanam, P. S., Polisetti, S. M., & Baadiga, R. (2025). Laboratory and Field Studies on Geogrid-Reinforced Pavements: Performance Evaluation and Carbon Footprint Analysis. *Indian Geotechnical Journal* (in press). <https://doi.org/10.1007/s40098-025-01291-7>
- [20] Quantifying the Effect of Geogrids in Asphalt Pavement Foundation Layers, *Materials and Construction*, 2022. <https://lnk.ink/rwqHI>
- [21] Sonawane, S.K., Dwivedi, A.K. & Naktode, P.L. Performance of coal ash based hot mix asphalt - an experimental investigation (2025). *Innov. Infrastruct. Solut.* 10, 274. <https://doi.org/10.1007/s41062-025-02087-7>